

A Fair OR–ML Framework for Resource Substitution in Large-Scale Networks

Ved Mohan,^{1,*} El Mehdi Er Raqabi,¹ Pascal Van Hentenryck¹

¹ *H. Milton Stewart School of Industrial and Systems Engineering, Georgia Institute of Technology, Atlanta, USA*

** Corresponding Author: vedmohan@gatech.edu*

Abstract

Ensuring that the right resource is available at the right location and time remains a major challenge for organizations operating large-scale logistics networks. The challenge comes from uneven demand patterns and the resulting asymmetric flow of resources across the arcs, which create persistent imbalances at the network nodes. Resource substitution among multiple, potentially composite and interchangeable, resource types is a cost-effective way to mitigate these imbalances. This leads to the resource substitution problem, a complex optimization problem both in theory and practice, which aims at determining the minimum number of resource substitutions from an initial assignment to minimize the overall network imbalance. In decentralized settings, where distributed schedulers pursue local objectives, achieving globally coordinated solutions becomes even more difficult. When substitution entails costs, effective prescriptions must also incorporate fairness and account for the individual preferences of schedulers.

This paper presents a generic framework that combines operations research (OR) and machine learning (ML) to enable *fair* resource substitution in large networks. The OR component models and solves the resource substitution problem under a fairness lens. The ML component leverages historical data to learn schedulers' preferences, guide intelligent exploration of the decision space, and enhance computational efficiency by dynamically selecting the top- κ resources for each arc in the network. The framework produces a portfolio of high-quality solutions from which schedulers can select satisfactory trade-offs. The proposed framework is applied to the network of one of the largest package delivery companies in the world, which serves as the primary motivation for this research. Computational results demonstrate substantial improvements over state-of-the-art methods, including an 80% reduction in model size and a 90% decrease in execution time while preserving optimality.

Keywords: mixed-integer programming, machine learning, large-scale optimization, resource allocation, fairness

1 Introduction

A major challenge faced by many organizations operating in large networks is to ensure that the right resource is available at the right location and at the right time. Achieving such allocation is complex partly because the flow of products within the network creates an imbalance. Any mileage between nodes that does not generate revenue, often called *deadhead* or *empty* miles, inflates costs and reduces productivity. Deadhead mileage across the American trucking industry was 16.3 percent of total mileage in 2023 ([ATRI, 2024](#)). Decision makers are forced to make empty moves to reposition resources. Heavy-duty trucks, including long-haul vehicles, account for approximately 25% of carbon dioxide emissions from U.S. transportation, despite comprising only about 10% of vehicles on the road ([Leslie and Murray, 2024](#)). Against this background, resource substitution among multiple, potentially composite and interchangeable, resource types emerges as an efficient solution, creating a win–win–win opportunity: it enables timely product delivery, supports real-time operational decisions, and reduces carbon impact. When compared with empty resource moves, resource substitution is highly preferred since it incurs no additional operating cost.

This paper studies the resource substitution problem in large networks. It addresses two complexities: (i) the resource substitution can only happen among interchangeable resources, and (ii) a solution that maximizes global utility may not be acceptable because its implementation costs can be unfairly distributed among schedulers. Thus, this paper studies resource substitution under the *fairness* lens. Real-world examples include fleet reassignment in airlines ([Jarrah et al., 2000](#)), containers repositioning in shipping yards ([Lin et al., 2015](#)), and bike rebalancing ([Dell'Amico et al., 2014](#)), all of which are shown to be NP-hard. Although optimal solutions to these substitution problems can theoretically be computed, practical execution frequently depends on distributed decision making by schedulers, complicating the implementation of centralized plans. This is particularly true when performance incentives are tracked at the scheduler level rather than globally.

This research is motivated by real-world business challenges. The need for substitution arises when the flow of products using resources (equipment) creates an imbalance within a large network from one week to another, mismatching the projected inventory levels. One way to measure equipment imbalance is to compute the difference between the inventory of each equipment type at each node at the start and end of the week. Then, a surplus or deficit (positive or negative change)

in the inventory level of a specific equipment type at a specific node is called an imbalance, and the total imbalance can be assessed by summing the absolute values of the imbalances for all equipment types at all nodes over the given time horizon (e.g., a week). To tackle this imbalance, the resource substitution typically occurs weekly upon the release of the upcoming week’s schedule. This paper studies resource balancing in networks via resource substitution. The primary objective is to minimize total network imbalance. Secondary objectives include achieving this with as few resource substitutions as possible and ensuring fair recommendations that support decentralized execution of a centralized policy, benefiting all stakeholders (e.g., end-users and schedulers).

The main contributions of this paper are summarized as follows:

1. **A general framework for fair resource substitution in large networks.** The paper proposes a framework that integrates operations research (OR) and machine learning (ML) to generate a portfolio of substitution recommendations for decision-makers.
2. **An OR component that models fairness explicitly.** The OR component models the resource substitution with fairness as a metric, and solves the problem using OR techniques. It overcomes key limitations of standard mixed-integer programming (MIP) formulations for resource substitution. The fairness metric emphasizes equitable substitutions between decentralized schedulers of a centralized policy.
3. **An ML component that leverages historical data.** The ML component leverages historical data to capture latent trends and scheduler preferences, enabling intelligent exploration of the decision space under a fairness perspective. It dynamically identifies the top- κ candidate resources for each arc, thereby reducing the search space of the OR model and improving both solution quality and computational efficiency.
4. **Application to a real-world large-scale network.** The framework is applied to one of the largest package delivery companies in the world, which motivated this study. Computational experiments on realistic instances demonstrate substantial benefits compared with existing substitution-based resource allocation methods (Yang et al., 2022). By integrating machine learning and operations research components, the framework reduces problem size by over 80% while preserving optimality, alongside a 90% decrease in execution time. This highlights the framework effectiveness in enhancing both computational efficiency and scalability in large-

scale operational contexts.

The remainder of this paper is structured as follows. Section 2 discusses the literature review. Section 3 presents the general framework. Section 4 highlights the case study from the industrial partner, while Section 5 concludes the paper.

2 Literature Review

This section reviews the relevant literature in three parts: resource reallocation, fairness in optimization, and the integration of ML and OR.

2.1 Resource Reallocation

Resource reallocation, also referred to as resource repositioning or redistribution, has been extensively studied, particularly within the context of freight transportation. Early research by [Leddon and Wrathall \(1967\)](#), [Misra \(1972\)](#), and [White \(1972\)](#) developed deterministic models for the repositioning of rail cars and containers under complete information about future demand. More recent studies have incorporated repositioning decisions jointly with load assignments to address larger-scale and more realistic operational settings ([Abrache et al., 1999](#); [Erera et al., 2005](#)). However, deterministic approaches are highly dependent on the accuracy of demand forecasts, which limits their robustness in uncertain environments ([Powell, 1986, 1987](#); [Crainic et al., 1993](#); [Yang et al., 2022](#)).

Repositioning has also been extensively examined in the bike-sharing literature, where spatially imbalanced flows between stations create persistent supply–demand mismatches. Prior studies have investigated efficient and cost-effective strategies for fleet management to meet anticipated demand ([Nair and Miller-Hooks, 2011](#); [Shu et al., 2013](#); [Bruglieri et al., 2014](#)). Dynamic repositioning in this context is often guided by heuristic or rule-based methods ([Ghosh et al., 2017](#); [Li et al., 2018](#)). More recent contributions have introduced clustering-based approaches for efficient routing ([Lv et al., 2020](#)), incentive-based rebalancing schemes that leverage user participation ([Chung et al., 2018](#)), and advanced heuristics that outperform traditional MIP formulations in both scalability and solution quality ([Schuijbroek et al., 2017](#); [Freund et al., 2022](#)).

Empty resource repositioning strategies can generally be classified into decentralized and centralized models. In decentralized frameworks, individual facilities or depots make independent decisions to optimize local fleet performance. For instance, [Du and Hall \(1997\)](#) developed a decentralized stock control policy for fleet sizing and repositioning within a terminal system, while [Song \(2005\)](#) analyzed container arrivals and repositioning decisions in a two-depot setting. Conversely, centralized models optimize decisions across the entire service network to enhance system-wide performance metrics ([Jansen et al., 2004](#)).

Because demand uncertainty critically influences repositioning efficiency, recent work has incorporated stochastic optimization techniques. [Erera et al. \(2009\)](#) proposed robust strategies to hedge against uncertainty, and [Long et al. \(2012\)](#) applied two-stage stochastic programming to manage variability in container demand and supply.

2.2 Fairness

Fairness has emerged as a major concern in contemporary decision-making problems ([Lodi et al., 2024](#)) and has gained growing attention within the OR community (for a recent survey, see [Chen and Hooker, 2023](#)). Efforts have increasingly focused on translating fairness principles into practical optimization frameworks applicable to real-world contexts such as supply chains and scheduling ([Chen and Hooker, 2022](#)).

[Bertsimas et al. \(2011\)](#) introduced the Price of Fairness (PoF), which measures the efficiency loss incurred when fairness constraints are imposed on optimal solutions. Building on this idea, [Karsu and Morton \(2015\)](#) and [Gupta et al. \(2023\)](#) examined fairness through equity and balance metrics, offering models that explicitly trade off efficiency for more equitable outcomes. More recently, [Yu et al. \(2025\)](#) extended these concepts to two-agent scheduling problems, analyzing outcomes through the lenses of proportionality, envy-freeness, and social welfare.

However, fairness has received comparatively less attention in the context of equipment substitution and resource allocation. Decentralized models tend to promote local fairness by granting individual terminals greater control over their own resources. In contrast, centralized models, while often more efficient from a system-wide perspective, can inadvertently create local imbalances by optimizing solely for global objectives. [Xie et al. \(2017\)](#) emphasized that this trade-off parallels

coordination challenges commonly observed in distributed logistics and game-theoretic frameworks, particularly in intermodal transport systems.

2.3 Machine Learning for Optimization

ML has been increasingly adopted to enhance operations research (OR) methodologies (for recent surveys, see [Bengio et al., 2021](#); [Scavuzzo et al., 2024](#)). Although the literature spans overlapping categories, such as solver acceleration, heuristic decision-making, and learning-based optimization, there is broad consensus on the growing synergy between ML and OR. A central objective in this integration is to leverage learned policies and value functions to replace manually designed heuristics within optimization algorithms. By framing optimization problems as data instances, researchers aim to enable cross-instance generalization, allowing models trained on specific problem distributions to improve decision quality and computational efficiency across similar problem classes.

Recent studies have demonstrated the potential of ML to accelerate and enhance optimization processes. [Tahir et al. \(2021\)](#) showed that neural networks trained on historical optimal or near-optimal solutions can improve both solution quality and computational time. In particular, neural architectures are used to predict which variables or constraints are most promising to include or exclude during the solution process, thereby guiding solver decisions. Similarly, [Morabit et al. \(2021\)](#) demonstrated that supervised learning can effectively guide column selection in column generation frameworks, allowing solvers to focus on the most promising variables. This concept was later extended by [Morabit et al. \(2023\)](#) to arc selection in constrained shortest path problems, where ML models predicted correct arcs, substantially reducing the search space in complex scheduling and routing applications.

In the context of supply chain resilience, [Er Raqabi et al. \(2024\)](#) proposed a generic and scalable re-optimization framework designed to address perturbations caused by global disruptions. Their deep neural network architecture reduces the number of complicating variables, achieving roughly 20% improvement in computational efficiency. More recently, [Akhlaghi et al. \(2025\)](#) introduced PROPEL, an integrated ML-OR framework for large-scale Supply Chain Planning (SCP). PROPEL employs a two-stage strategy: supervised learning is used to predict integer variables that can be fixed to zero, while deep reinforcement learning (DRL) selectively relaxes these decisions to enhance

solution quality. This approach has shown remarkable computational benefits, achieving up to 88% reduction in primal gap and a 13–15 \times improvement in performance on industrial-scale SCP problems involving millions of variables.

2.4 Paper Positioning

This paper investigates optimization strategies for centralized policy design combined with decentralized execution across multiple jurisdictions. Each jurisdiction, managed by a local network scheduler, comprises resource nodes that enable opportunities for inter-jurisdictional collaboration and coordination.

From a fairness perspective, this study extends substitution-based approaches in the literature (Yang et al., 2022) by explicitly integrating fairness considerations into both the OR and ML components. The objective is to develop resource reallocation plans that are not only computationally efficient but also equitable across locations and fair to individual decision makers involved in decentralized execution.

While prior studies in related domains, such as airline planning, where the top- κ flights following a given flight are considered (Quesnel et al., 2022), and vessel assignment, where the top- κ quays are evaluated for each vessel (Er Raqabi et al., 2024), have relied on static values of κ , their static approaches do not account for the structural context of individual arcs within the network. This work introduces a dynamic top- κ_a mechanism for each arc $a \in \mathcal{A}$, in which κ_a is adapted based on the betweenness centrality of each arc (Newman, 2018), enabling a context-sensitive reduction of the search space. Thus, κ varies across arcs according to their structural characteristics, quantified through an arc betweenness metric that reflects their relative importance in the network.

The proposed dynamic top- κ approach represents a novel contribution not only to the resource substitution literature but also to the broader class of optimization problems that couple operations research with data-driven learning. By adapting κ based on network structure and contextual features, this mechanism introduces a generalizable principle for adaptive search-space reduction in hybrid OR–ML frameworks, with potential applicability to other domains such as airline scheduling, maritime logistics, and transportation planning.

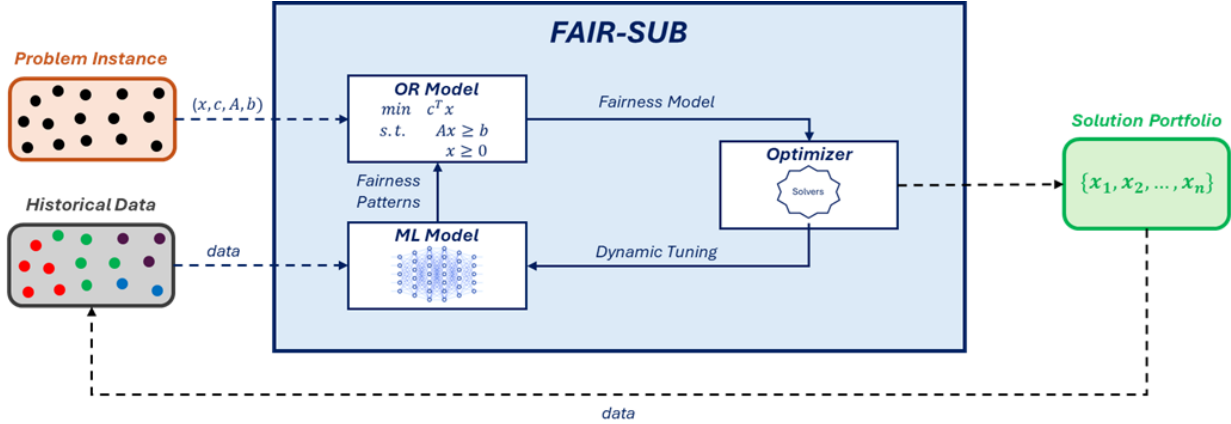


Figure 1: The Fairness Framework.

3 General Framework

This section introduces the proposed fairness framework before detailing the OR component, the ML component, and the solution portfolio.

3.1 Fairness Framework Description

The proposed fairness framework for resource substitution, referred to as *FAIR-SUB* and depicted in Figure 1, takes as input both the problem instance and relevant historical data, and outputs a solution portfolio for local scheduler(s). The problem instance serves as the basis for constructing the OR model, while the historical data is used by the ML model to extract insights that support the OR formulation. The strengths of both models are integrated through an *optimizer*, which represents the collection of computational techniques used to tackle large-scale optimization problems (Er Raqabi et al., 2025). These include metaheuristics (Er Raqabi et al., 2023b), exact algorithms (Er Raqabi et al., 2023a), and commercial or open-source solvers (Himmich et al., 2023).

A key aspect of the FAIR-SUB framework is that both the OR and ML components explicitly account for fairness. In the OR model, fairness is embedded in the objective function through established metrics from the literature (Chen and Hooker, 2023). In parallel, the ML model implicitly captures fairness by learning from historical scheduler preferences and patterns, ensuring that the resulting recommendations balance efficiency and fairness. The optimizer feedback can be used to tune the ML model dynamically. The solution portfolio is added to the historical data.

3.2 The OR Component

The resource substitution problem is formally defined as follows. Consider a directed graph $\mathcal{G} = (\mathcal{N}, \mathcal{A})$, where \mathcal{N} is the set of nodes and \mathcal{A} is the set of arcs. Each arc $a \in \mathcal{A}$ corresponds to a task to be performed by an allocated resource $r \in \mathcal{R}$. When the available resources are performing the tasks (e.g., flow through the network) over a given planning horizon, an imbalance might occur within each node. Let $A_n^+ = \{(i, n) : i \in \mathcal{N}\}$ (resp. $A_n^- = \{(n, i) : i \in \mathcal{N}\}$) the set of incoming (resp. outgoing) arcs at node $n \in \mathcal{N}$. A resource assignment is a function $\Phi : \mathcal{A} \rightarrow \mathcal{R}$ that assigns a resource to each arc and the initial resource assignment is denoted Φ_0 . The imbalance of an assignment Φ can be computed as follows:

$$\mathcal{I}(\Phi) := \sum_{r \in \mathcal{R}} \sum_{n \in \mathcal{N}} \left| \sum_{a \in A_{nr}^+} \mathbb{1}(\Phi_0(a) = r) - \sum_{a \in A_{nr}^-} \mathbb{1}(\Phi_0(a) = r) \right|.$$

FAIR-SUB tackles the imbalance problem by substituting resources within the arcs of network. It consists of two stages. Stage 1 computes the minimal imbalance I^* of the network. An assignment Φ is optimal when $\mathcal{I}(\Phi) = I^*$. Stage 2 computes the optimal Φ^* that is closest to Φ_0 , i.e., $\Phi^* \in \arg \min_{\mathcal{I}(\Phi)=I^*} \|\Phi - \Phi_0\|$, where $\|\Phi - \Phi_0\| = |\{a \in \mathcal{G} : \Phi(a) \neq \Phi_0(a)\}|$.

Denote by \mathcal{R}_a the set of resources that can be used on arc $a \in \mathcal{A}$ (i.e., the resources that can perform the corresponding task). The decision variables of Stage 1 are

$$x_{ar} = \begin{cases} 1, & \text{if resource } r \text{ is used on arc } a, \\ 0, & \text{otherwise.} \end{cases} \quad (3.1)$$

and $I_{nr} \geq 0$ captures the imbalance of resource r at node n . The Stage 1 model is defined as follows:

$$I^* = \min \sum_{n \in \mathcal{N}} \sum_{r \in \mathcal{R}} I_{nr} \quad (3.2)$$

$$s.t. \quad \sum_{a \in \mathcal{A}_n^+} x_{ar} - \sum_{a \in \mathcal{A}_n^-} x_{ar} \leq I_{nr}, \quad \forall n \in \mathcal{N}, \quad (3.3)$$

$$\sum_{a \in \mathcal{A}_n^-} x_{ar} - \sum_{a \in \mathcal{A}_n^+} x_{ar} \leq I_{nr}, \quad \forall n \in \mathcal{N}, \quad (3.4)$$

$$\sum_{r \in \mathcal{R}_a} x_{ar} = 1, \quad \forall a \in \mathcal{A}, \quad (3.5)$$

$$x_{ar} \in \{0, 1\}, \quad \forall a \in \mathcal{A}, r \in \mathcal{R} \quad (3.6)$$

Objective (3.2) minimizes the total imbalance. Constraints (3.3) and (3.4) ensure that the imbalance within each node for each resource is equal to the net surplus or deficit of that resource at that node. Constraints (3.5) ensure the assignment of exactly one resource to each arc.

The Stage 2 model minimizes the number of changes Δ^* , and with Constraints (3.8), ensures the obtained resource substitution is optimal:

$$\Delta^* = \min \sum_{a \in \mathcal{A}} (1 - x_{a\Phi_0(a)}) \quad (3.7)$$

$$s.t. \quad \sum_{n \in \mathcal{N}} \sum_{r \in \mathcal{R}} I_{nr} \leq I^*, \quad (3.8)$$

(3.3) to (3.6).

While this approach allows for finding the minimal imbalance I^* and the minimal number of changes Δ^* to bring balance back to the network, it might not be fair for all the schedulers involved. A *scheduler* is a decision maker in charge of a set of nodes within the network. Some schedulers may be required to implement disproportionately more changes. Some manage large or high-throughput areas; others oversee fewer nodes with intense volume. Coordination practices also vary: some collaborate regularly with neighbors, while others operate in relative isolation. Formally, let \mathcal{S} be the set of schedulers for network \mathcal{G} , and \mathcal{N}_s be the set of nodes corresponding to scheduler $s \in \mathcal{S}$. To incorporate fairness, the objective function in Stage 2 is modified to reflect one of the fairness metrics proposed in the literature (Chen and Hooker, 2023): the *Minimax* metric that minimizes the maximum changes per schedule. Let $A_s = \{(i, j) : i, j \in \mathcal{N}_s\} \cup \{(i, j) : i \in \mathcal{N}_s, j \notin \mathcal{N}_s\}$, i.e., the arcs corresponding to scheduler s are the arcs between their nodes and the arcs outgoing from one of their nodes to nodes assigned to different schedulers. Stage 2 model becomes

$$\Delta^{fair} = \min_{s \in \mathcal{S}} \max_{a \in \mathcal{A}_s} (1 - x_{a\Phi_0(a)}) \quad (3.9)$$

$$s.t. \quad \sum_{n \in \mathcal{N}} \sum_{r \in \mathcal{R}} I_{nr} \leq I^*, \quad (3.10)$$

(3.3) to (3.6).

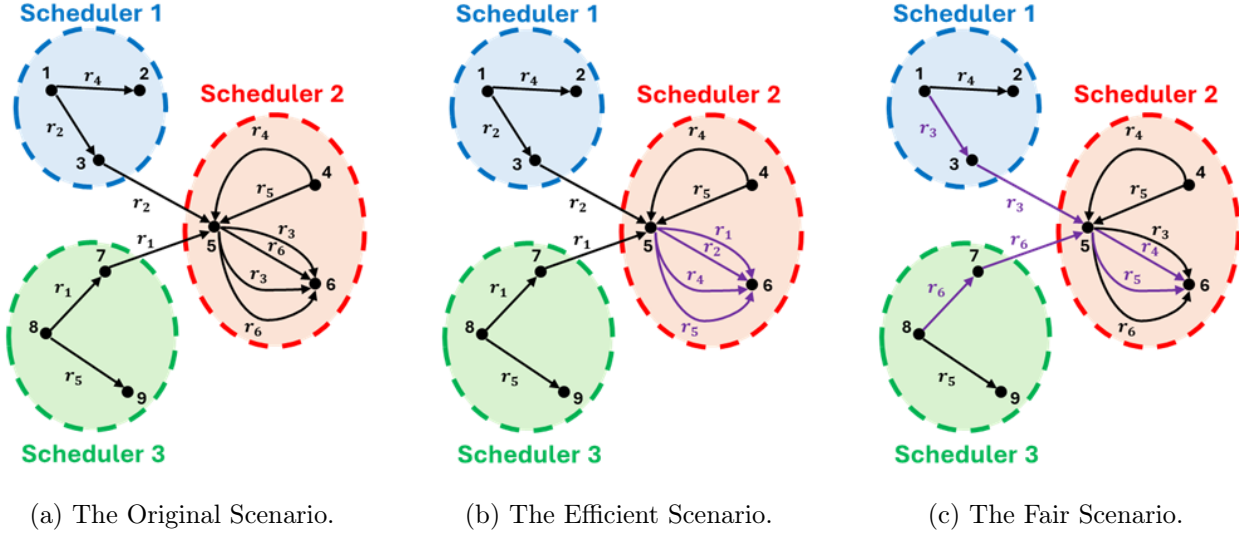


Figure 2: Example with 6 Resources and 3 Schedulers operating 3 Nodes Each.

This model can be linearized as follows

$$\Delta^{fair} = \min Z \quad (3.11)$$

$$s.t. Z \geq \sum_{a \in \mathcal{A}_s} (1 - x_{a\Phi_0(a)}), \quad \forall s \in \mathcal{S}, \quad (3.12)$$

(3.3) to (3.6), (3.10).

The following example compares the efficient and fair models.

Example 1. Figure 2 presents a scenario with six resources (r_1-r_6) and three schedulers (s_1-s_3), each operating three nodes. As shown in Figure 2a, the initial imbalance is 20, while the minimal achievable imbalance is 12. To illustrate the reallocation required to attain this minimal imbalance, Figures 2b and 2c depict two scenarios corresponding to Models (3.7) and (3.9), respectively. Changes relative to the original configuration are highlighted in purple.

When considering efficiency, the model reaches the minimal imbalance by substituting 4 resources on the arcs corresponding to scheduler 2. No changes are required for the other two schedulers. When considering fairness, the model reaches the minimal imbalance by substituting 2 resources on the arcs corresponding to each of the three schedulers. In a collaborative environment, the fair scenario is more implementable since all schedulers have 2 substitutions each, compared to only one scheduler having 4 substitutions.

The OR models above focus on two primary objectives: (i) minimizing network imbalance in Stage 1 and (ii) limiting the number of resource changes in Stage 2. These quantities serve as the operational “costs” relevant to the decision-making setting studied. Without loss of generality, this model considers the number of changes and the total network imbalance as the only cost components, which allows us to isolate and analyze the structural properties of the resource substitution problem.

That said, the proposed framework is flexible and can accommodate richer cost structures. In particular, arc-dependent substitution costs, such as the cost of deploying a super-long resource instead of a short one, or distance-based penalties along the arc, can be incorporated directly into the objective or as additional constraints.

3.3 The ML Component

Using historical operational data collected by companies, it is possible to develop ML models that learn schedulers’ preferences (Bengio et al., 2021), thereby promoting fairness in decision making. Such models help uncover latent patterns and behavioral trends that can enhance both the OR model and the optimizer’s performance. To construct these ML models, it is essential to specify the target variable, define the historical data structure, identify relevant features, and determine the network architecture. While numerous machine learning techniques apply to this task, the following approach is designed to address the specific structure and requirements of the resource substitution problem.

Target. In the resource substitution framework, the ML component aims at estimating the likelihood that a specific resource $r \in \mathcal{R}$ be assigned to an arc $a \in \mathcal{A}$. Formally, the model predicts probabilities p_{ar} representing the propensity of resource r to fulfill the task associated with arc a . These estimates are then used to identify the most promising candidates by selecting the top κ resources for each arc, where κ denotes an integer cut-off parameter. By focusing only on these high-probability resource–arc pairs, the ML component effectively reduces the decision space of the optimization models in Stage 1 (Model 3.2) and Stage 2 (Model 3.9), thereby decreasing the number of binary decision variables x_{ar} to be considered. For each arc a , the model produces a probability vector $Y_a \in \mathbb{R}^{|\mathcal{R}|}$, where the r -th entry corresponds to p_{ar} . Sorting Y_a in descending order of p_{ar} enables the extraction of the top- κ resources, which are subsequently used as the candidate set for

substitution decisions.

Unlike prior approaches that adopt a fixed, static κ across all arcs, this study introduces a dynamic top- κ_a mechanism, in which κ_a is determined adaptively based on each arc's betweenness centrality (Newman, 2018). Arcs with high betweenness, indicating strong structural importance and greater potential for flow interaction, are assigned larger κ_a values, allowing for broader exploration of substitution options. Conversely, arcs with low betweenness receive smaller κ_a values, emphasizing computational efficiency in regions where local changes have limited impact. This dynamic treatment of κ_a ensures that the reduction of the search space is both context-aware and structurally informed, enhancing scalability while maintaining fairness and solution optimality.

The structural importance of each arc $a \in \mathcal{A}$ is quantified using its *betweenness centrality*, denoted by $B(a)$, and specified as

$$B(a) = \sum_{\substack{i,j \in \mathcal{N} \\ i \neq j}} \frac{\sigma_{ij}(a)}{\sigma_{ij}}, \quad (3.13)$$

where σ_{ij} is the total number of shortest paths between nodes i and j , and $\sigma_{ij}(a)$ is the number of those paths that pass through arc a . A higher $B(a)$ indicates that arc a is more frequently used as a connector between node pairs, reflecting its structural importance.

Based on their betweenness values, arcs are categorized into three classes:

1. **Low-betweenness arcs** ($B(a) < \tau_1$): peripheral connections;
2. **Medium-betweenness arcs** ($\tau_1 \leq B(a) < \tau_2$): moderately connected links;
3. **High-betweenness arcs** ($B(a) \geq \tau_2$): major connectors or bottlenecks in the network.

These classes inform the assignment of dynamic top- κ_a values. Specifically, high-betweenness arcs are allocated larger κ_a values to allow for broader exploration of substitution options, while low-betweenness arcs receive smaller κ_a .

Data & Features. The data used for training the ML model depends on the specific application context. Once the historical data is identified, appropriate features are selected to construct the feature vector X_{ar} for each arc $a \in \mathcal{A}$ and resource $r \in \mathcal{R}$. In general, features may include network-related attributes (e.g., origin and destination nodes), operational responsibilities (e.g., schedulers associated with each node), and task characteristics (e.g., quantity, time of day, duration).

Network Architecture. Given the richness of the available data, each observation is represented by a high-dimensional feature vector. In such settings, individual features often exhibit weak correlation with the prediction target, implying that accurate forecasting requires a model capable of capturing complex, nonlinear interactions among features. Deep neural networks (DNNs) are particularly well-suited to this task due to their ability to learn hierarchical representations from data (Goodfellow et al., 2016; LeCun et al., 2015). A DNN consists of multiple layers of interconnected computational units, or neurons. The input layer encodes the explanatory features, while the output layer produces the predicted probability p_{ar} associated with assigning resource $r \in \mathcal{R}$ to arc $a \in \mathcal{A}$. Between these layers, one or more hidden layers enable the model to capture intricate relationships between the inputs and outputs. Each neuron applies a weighted linear combination of its inputs, followed by a nonlinear activation function, which allows the network to approximate complex functional mappings. During the training phase, the model iteratively adjusts its weights and activation parameters to minimize prediction error over the training dataset. Once trained, the DNN can estimate p_{ar} for unseen data instances, providing a scalable and flexible mechanism for predicting resource–arc preferences across large transportation networks.

3.4 Solution Portfolio

Once the OR and ML models are designed, it is possible to combine the ML insights generated from the historical data with the OR models to boost the optimizer’s performance in solving the OR models. While the solving might be quick and optimal, it might also take more time than expected, especially in large-scale contexts, which require additional computational strategies. In such contexts, it is advisable to employ established mathematical optimization strategies from the literature, including metaheuristics, decomposition approaches, and parameter tuning of the underlying MIP solver. Examples include: (1) the iterated local search metaheuristic, which starts from the initial assignment Φ_0 and explores solutions around it locally to find resource substitutions that decrease the imbalance (Lourenço et al., 2003); (2) the Dantzig-Wolfe decomposition, which starts with an initial set of x_{ar} variables and uses column generation to identify and add more promising x_{ar} variables (Desaulniers et al., 2006); (3) the parameter configuration, which consists of using available tuners in the literature to identify better configurations than the default configuration of the considered solver on the given problem instance (López-Ibáñez et al., 2016; Himmich et al.,

2023).

Although only two formulations are illustrated here (the efficient and minimax models), the same framework can be extended to evaluate numerous formulations under different fairness metrics. (Chen and Hooker, 2023). After solving the problem using the various formulations, the suggestion is to provide the schedulers with a portfolio of solutions from which they can choose. This portfolio contains a set of Pareto-optimal solutions that might not be optimal from a solver perspective, but ensure a fair resource substitution in the considered network \mathcal{G} (Bertsimas et al., 2011).

Beyond offering a set of Pareto-efficient trade-offs, the solution portfolio also provides interpretable and actionable recommendations for the schedulers. Each substitution suggested within the portfolio can be classified as either an *internal substitution* or a *collaborative substitution*. Internal substitutions occur between two nodes managed by the same scheduler and reflect opportunities for local reallocation of resources within a single operational jurisdiction. In contrast, collaborative substitutions involve arcs linking nodes managed by different schedulers, thereby promoting cross-scheduler coordination and network-level efficiency. This classification allows decision makers to understand whether improvements arise from local flexibility or inter-scheduler collaboration, enabling more informed and context-aware decision support in real-world scheduling environments.

4 Package Delivery Company Case Study

This section presents a case study conducted with a package delivery company. The operational context is described first, followed by a detailed explanation of the experimental design used to evaluate the proposed framework and the corresponding computational results. The section concludes with a discussion of the managerial insights derived from the analysis, emphasizing the implications for both operational efficiency and fairness in resource allocation.

4.1 Problem Description

The case study investigated in this paper focuses on a resource substitution problem encountered by a major package delivery company. In this context, packages are transported between facilities and customers through a large network of interconnected terminals. Each week, the company must allocate and position equipment across facilities to meet anticipated package flows for the

upcoming period. This planning task is complicated by network imbalances, forcing schedulers to reposition equipment: an empty, costly, and non-productive operation. Efficient resource allocation and substitution decisions play a crucial role in ensuring on-time deliveries, supporting operational decision making, and minimizing the environmental footprint associated with empty movements.

One approach to measuring equipment imbalance is to consider differences in the inventory of different equipment types at a facility at the start of the week and at the end of the week. A surplus or deficit (positive or negative change) in the inventory level of a specific equipment type at a specific terminal is called an imbalance, and the total imbalance of a plan can be assessed by summing the absolute values of the imbalances for all equipment types at all terminals. Equipment substitution complements the empty repositioning of equipment, but it is only possible if companies operate multiple, interchangeable equipment types. When compared with repositioning empty equipment, equipment substitution may be preferred since this may not require any additional operating cost. The company operates several equipment types, which can be grouped into 3 groups: trailers with a length of 28 feet called shorts, trailers with a length ranging from 40 to 48 feet called longs, and trailers with a length of 53 feet called extra-longs. These can be composite and are mostly interchangeable (see Appendix A where all the substitution matrix for all equipment types is given).

The balancing process occurs weekly with the release of the schedule for the upcoming week. Schedulers aim at minimizing net imbalances within their facilities (nodes), often referred to as “one in, one out.” Schedulers may be responsible for various facility types: hubs (large and centralized facilities that handle high volumes of shipments and serve as major distribution points in the network), centers (mid-sized facilities that coordinate regional operations), and locals (small facilities focused on last-mile delivery and direct customer interactions within a limited geographic area). A given jurisdiction may contain up to 90 facilities, with cooperation between connected jurisdictions. Connectivity between each pair of nodes is not guaranteed.

4.2 Experimental design

This section describes the test instances and the ML model used in the experiments. Both the OR and ML components are implemented in Python, and optimization experiments are solved using Gurobi version 12.0.2. All computations were performed on a 40-core machine with 384 GB of

Class	# Sched.	# Nodes	# Arcs	# Equip.	I_0
1	2	167	138992	13	4236
2	5	356	509557	16	10644
3	8	536	893028	17	18370
4	11	612	1278907	18	22733
5	15	709	1816934	19	28879
6	20	974	3004375	20	40799
7	30	1296	5259231	22	58630
8	40	1588	8341357	23	78488

Table 4.1: Instances

RAM, running Oracle Linux Server 7.7 on a 3.20 GHz Intel® Core™ i7-8700 processor. The ML models are implemented using the PyTorch library. For evaluation, real-time runtime is reported to assess computational performance across all test instances.

4.2.1 Instances

The case study is based on eight classes of real-world problem instances supplied by one of the largest package delivery companies in the world. Key characteristics of these instances include the number of schedulers, nodes, arcs, equipment, and the initial network imbalance. For each class, 10 instances are generated, resulting in a total of 80 test cases. The average values of these features for each class are summarized in Table 4.1.

For brevity, only average results for each class are reported, while instance-level results are provided in the Online Supplement.

4.2.2 Machine Learning Model

The deep neural network (DNN) is trained to predict the most probable equipment type associated with each origin–destination (O–D) movement. As described in Section 3, the ML component constructs a probability vector Y_a for every arc $a \in \mathcal{A}$, where each entry corresponds to the likelihood of assigning a specific resource $r \in \mathcal{R}$. The model is developed within a supervised learning framework using data derived from previously implemented solutions, hereafter referred to as *reference*

solutions. Each reference solution \bar{x} specifies one resource assignment per arc, thereby yielding $|A_{\bar{x}}|$ training instances of the form (X_{ar}, y_{ar}) , with $a \in \mathcal{A}_{\bar{x}}$ and $r \in \mathcal{R}$. To enhance learning robustness, all equivalent optimal reference solutions are included in the training set by exploiting problem symmetries. This augmentation allows for multiple feasible assignments to be represented for a given arc a , capturing variability in optimal or near-optimal configurations. For each pair (a, r) , the associated label y_{ar} reflects the empirical frequency with which resource r is assigned to arc a across all reference solutions, thus encoding observed assignment patterns as probabilistic targets for model training.

Each arc $a \in \mathcal{A}_{\bar{x}}$ and resource $r \in \mathcal{R}$ have a feature vector X_{ar} , which contains the following features:

1. A categorical feature indicating the origin node, denoted $f^{(1)}$.
2. A categorical feature indicating the destination node, denoted $f^{(2)}$.
3. A numerical feature indicating the volume to be transported, denoted $f^{(3)}$.
4. A categorical feature indicating the scheduler in charge of the origin node, denoted $f^{(4)}$.
5. A categorical feature indicating the scheduler in charge of the destination node, denoted $f^{(5)}$.
6. A numerical feature corresponding to the time of the day, denoted $f^{(6)}$.
7. A numerical feature corresponding to the time of the week, denoted $f^{(7)}$.
8. A numerical feature corresponding to the miles between the origin and destination nodes, denoted $f^{(8)}$.
9. A categorical feature corresponding to the size of the equipment required to transport the volume, denoted $f^{(9)}$.

The DNN is trained using a pool of reference solutions compiled over a 13-week historical horizon. For each candidate pair (a, r) , the model learns to predict a label corresponding to the likelihood of assigning resource r to arc a . The predicted label for each input vector X_{ar} is denoted by y_{ar}^{prd} . To evaluate model generalization, the dataset of labeled pairs (X_{ar}, y_{ar}) is randomly partitioned into three mutually exclusive subsets: 60% for training, 20% for validation, and 20% for testing. The split is stratified by equipment class to ensure that the distribution of target labels is consistent across all subsets, thereby avoiding biased performance estimates for underrepresented classes. Once trained,

Category	Parameter	Value
Model Architecture	Hidden Layers	2
	Neurons (per layer)	[128, 64]
	Output Neurons	30
	Activation (Hidden/Output)	ReLU/Softmax
Training Configuration	Optimizer	Adam
	Learning Rate	0.001
	Dropout Rate	0.3
	Loss Function	Categorical Crossentropy
	Epochs/Batch Size	50/32
Data Splitting	Train/Test/Validation Ratio	60/20/20
	Stratification	Yes (by resource type)
Evaluation Metrics	Primary/Secondary	Loss/AUROC

Table 4.2: ML Model Hyperparameters and Training Configuration

the model produces a predicted probability y_{ar}^{prd} for each resource–arc pair. These predictions are then ranked in descending order to identify the most promising resource candidates for each arc. The resulting ranking enables the selection of the top- κ resources, which are subsequently passed to the OR component for substitution optimization.

The machine learning architecture employed is a fully connected feedforward DNN. Consistent with standard design principles, the number of neurons in each hidden layer is set to be less than or equal to that of the preceding layer, ensuring a gradually contracting structure. All hidden-layer neurons use the rectified linear unit (ReLU) activation function to introduce nonlinearity, while the output layer consists of a single sigmoid neuron, producing a probability value bounded within the interval $[0, 1]$. The model hyperparameters, including the number of hidden layers, neurons per layer, learning rate, and batch size, along with the training algorithm, are tuned via a randomized grid search (see Table 4.2). The final network configuration is selected based on its performance on the validation set.

The predictive performance of the ML model is evaluated by assessing how well the top-ranked κ resources correspond to the true labels across all arcs. Specifically, for each arc $a \in \mathcal{A}$, let $j \in 1, 2, \dots, \kappa$ denote the index of the j^{th} -ranked resource in the ordered prediction vector Y_a , where y_{ar_1} represents the highest predicted probability and y_{ar_κ} the κ^{th} . The model effectiveness is then quantified using the *label sum ratio*, computed as the proportion of true labels captured within

κ	1	2	3	4	5
Average TOP_κ	69.50%	87.20%	97.33%	99.10%	100.00%

Table 4.3: Average TOP_κ for the Test Pairs

the top- κ predictions. This measure reflects the model ability to rank the most relevant resource assignments at the top of the list, providing a direct and interpretable indicator of ranking accuracy.

$$TOP_\kappa = \frac{\sum_{a \in \mathcal{A}} \sum_{j=1}^{\kappa} y_{ar_j}}{\sum_{a \in \mathcal{A}} \sum_{r \in \mathcal{R}} y_{ar}}$$

The DNN is trained in a supervised setting using the Adam optimizer (Kingma and Ba, 2015), and multiple regularization mechanisms are incorporated to mitigate overfitting. Specifically, dropout is applied to hidden layers with probability 0.3. In addition, model performance, measured by the validation TOP_κ metric, is monitored every ten epochs. Training is halted early if validation performance declines for two consecutive evaluations or upon reaching a predefined maximum number of epochs.

The training process for the neural network required less than two hours. In practical applications, this computational cost is negligible, as each ML model is trained once and subsequently deployed for extended periods (e.g., several months or years). Moreover, retraining the model is substantially faster—typically a few minutes—since the network parameters start from a near-optimal configuration and only require fine-tuning. The performance of the trained model is summarized in Table 4.3. Each arc can correspond to multiple potential equipment types, and the network performance is evaluated for κ values ranging from 1 to 5. As discussed in Section 3.3, the choice of κ is guided by arc betweenness values, with a maximum value of 5.

The proposed ML model is employed to enhance both stages of the resource substitution framework. Unlike Yang et al. (2022), who rely on predefined compatibility matrices similar to the one presented in Appendix A, the proposed ML approach inherently satisfies compatibility constraints. Specifically, since the model is trained on historical data that only includes compatible equipment–arc pairings, it ensures that an arc’s initial equipment is substituted only with compatible alternatives. This data-driven formulation not only preserves operational feasibility but also leads to a substantial reduction in the number of arcs considered.

Class	# Sched.	# Nodes	# Arcs	# Equip.	# Inter.	# Collab.	I_0	I^*	Gain	Time
1	2	167	138992	13	138709	283	4236	3444	18.69%	1.02
2	5	356	509557	16	462500	47056	10644	8357	21.49%	3.13
3	8	536	893028	17	811401	81627	18370	14709	19.93%	5.53
4	11	612	1278907	18	1089299	189608	22733	17667	22.28%	7.61
5	15	709	1816934	19	1448200	368734	28879	22863	20.83%	9.57
6	20	974	3004375	20	2213879	790496	40799	32641	20.00%	13.19
7	30	1296	5259231	22	3516181	1743050	58630	47863	18.37%	19.77
8	40	1588	8341357	23	4910272	3431084	78488	65655	16.35%	26.48

Table 4.4: Minimal Imbalance from Stage 1

To prioritize substitutions where they have the greatest impact, directed edge betweenness centrality is computed on the network using a sampling-based approximation of k for scalability, and each movement is classified as High, Medium, or Low based on the tuned betweenness thresholds τ_1 and τ_2 . These thresholds were determined empirically through preliminary experiments. These exploratory runs were conducted on representative instances to identify breakpoints that yield balanced class distributions and stable performance across test cases. Next, the dynamic- κ mechanism is applied, where movements on high-betweenness corridors receive a larger κ value, movements on medium-betweenness corridors receive a medium κ value, and low-betweenness movements are restricted to lower κ values.

4.3 Computational Performance

This section evaluates the computational performance of the proposed framework across the eight problem classes introduced earlier. The experiments are designed to assess both the quality of the solutions and the efficiency gains achieved through the integration of the OR and ML components, particularly the dynamic top- κ_a mechanism.

Table 4.4 summarizes the Stage 1 results (minimal imbalance) for the eight classes. In addition to the already presented features, Table 4.4 reports the number of internal arcs (i.e., the arcs linking nodes for which the scheduler is the same), the number of collaborative arcs (i.e., arcs for the scheduler is not the same), the minimal imbalance (I^*), the reduction in imbalance (Gain), which is computed as $\frac{I_0 - I^*}{I_0}$, and the execution time (Time) in seconds.

Table 4.4 reveals that, as the size increases, so does the scale of the problem, which slightly impacts

Class	# Sched.	I_0	I^*	Efficiency			Fairness			$\Delta^{FAIR} - \Delta^*$	$Z^{FAIR} - Z^*$
				Δ^*	Z^*	Time	Δ^{FAIR}	Z^{FAIR}	Time		
1	2	4236	3444	321	199	1.44	357	188	1.53	35	11
2	5	10644	8357	952	354	4.74	1135	242	5.50	183	112
3	8	18370	14709	1542	452	8.27	1852	274	11.30	310	178
4	11	22733	17667	2048	443	12.25	2796	285	15.50	748	159
5	15	28879	22863	2701	486	15.14	4184	308	18.16	1483	178
6	20	40799	32641	3725	710	22.13	7350	397	24.98	3624	313
7	30	58630	47863	4941	688	34.99	9039	331	39.65	4098	357
8	40	78488	65655	5943	732	44.33	13510	394	53.11	7567	338

Table 4.5: Stage 2 for the Efficient and Fair Models

the computational effort, as seen in the longer execution times for Classes 7 and 8. Notably, the reduction percentage remains significant across all classes, indicating that the first stage reduces the imbalance regardless of problem size.

Table 4.5 presents results comparing the efficient and fair Stage 2 models across the eight classes. In addition to the previously described features, the analysis reports the number of changes (Δ), the maximum number of changes per scheduler (Z), and the execution time (Time) required by the second stage for both the efficient and fair models. The cost of fairness is defined as $\Delta^{FAIR} - \Delta^*$, while the gain in fairness is given by $Z^{FAIR} - Z^*$. The considered fairness metric is the *minimax* metric.

Across all classes, the fair model achieves a notable increase in fairness except for the first class. For other classes, the average gain in fairness goes from 112 to 357. This comes with a cost, which increases significantly with the size of the instances, with up to 7567 additional changes on average for class 8. As instance size and complexity grow, the trade-offs between fairness and the cost to achieve it become more pronounced. This suggests that the more collaborative arcs, the higher the potential of achieving more fairness among schedulers. Overall, these results indicate that while fairness can be effectively integrated, its cost varies depending on problem structure, and some instances allow fair outcomes without compromising efficiency.

Class	# Sched.	I ₀	I [*]	Efficiency ($\alpha = 0$)			$\alpha = 0.25$			$\alpha = 0.5$			$\alpha = 0.75$			Fairness ($\alpha = 1$)		
				Δ^*	Z^*	Time	$\Delta^{0.25}$	$Z^{0.25}$	Time	$\Delta^{0.50}$	$Z^{0.50}$	Time	$\Delta^{0.75}$	$Z^{0.75}$	Time	Δ^{FAIR}	Z^{FAIR}	Time
1	2	4236	3444	321	199	1.44	321	190	1.44	322	190	1.43	323	188	1.51	357	188	1.53
2	5	10644	8357	952	354	4.74	952	257	4.81	958	250	4.91	969	242	5.33	1135	242	5.50
3	8	18370	14709	1542	452	8.27	1542	303	9.30	1555	289	9.17	1574	276	9.28	1852	274	11.30
4	11	22733	17667	2048	443	12.25	2048	323	12.53	2057	314	13.03	2094	291	14.25	2796	285	15.50
5	15	28879	22863	2701	486	15.14	2701	360	15.98	2724	335	16.75	2754	311	17.04	4184	308	18.16
6	20	40799	32641	3725	710	22.13	3725	488	21.90	3764	443	21.85	3823	400	26.61	7350	397	24.98
7	30	58630	47863	4941	688	34.99	4941	428	33.89	4984	382	34.26	5041	341	37.58	9039	331	39.65
8	40	78488	65655	5943	732	44.33	5944	457	44.31	5970	425	47.86	6002	399	44.57	13510	394	53.11

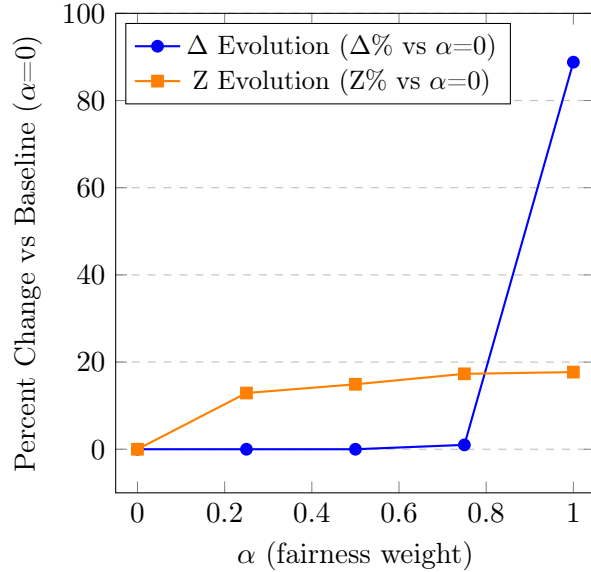
Table 4.6: Trade-off between Efficiency and Fairness

4.4 Trade-off Between Efficiency and Fairness

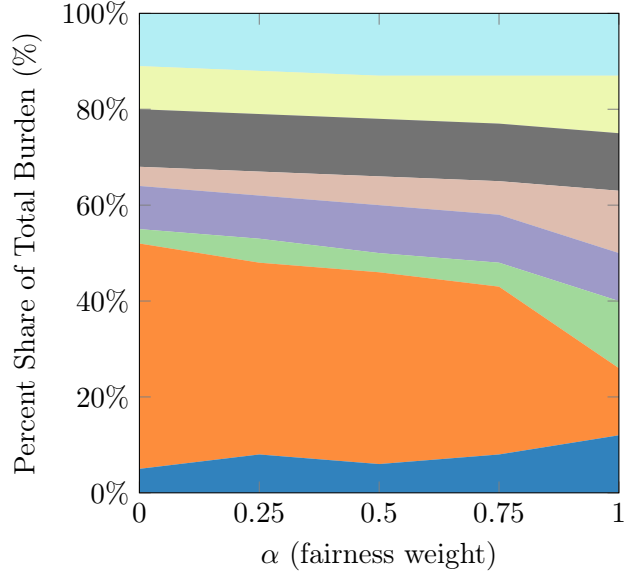
A weighted-objective model is also implemented, in which α represents the weight assigned to the efficient objective and $1 - \alpha$ corresponds to the weight assigned to the fair objective. Table 4.6 shows the results for various values of α . The results show that as α increases from 0 to 1, the focus shifts from minimizing total changes (Δ) to limiting the maximum disruption for any scheduler (Z^*). In Class 1, Δ increases from 321 at $\alpha = 0$ to 357 at $\alpha = 1$. In comparison, Z^* decreases from 199 to 188 for intermediate values but does not improve under full fairness, indicating diminishing returns for fairness improvement. In Class 8, the total changes rise significantly from 5943 to 13510 as fairness becomes dominant, while Z^* stabilizes at 394. This pattern highlights the cost of fairness: reducing the worst-case burden for individual schedulers requires spreading disruptions more widely, inflating the overall number of changes.

Execution time exhibits a clear dependency on both class size and fairness requirements. For Class 1, runtime remains relatively stable (less than 2 seconds) across all α values, implying that fairness enforcement is computationally inexpensive in small systems. However, in Class 8, where the number of schedulers and complexity increase, execution time grows as α approaches 1. This indicates that incorporating fairness constraints in large-scale scheduling not only raises the total number of changes but also increases computational effort. Overall, the table underscores that fairness reduces the burden on the most affected scheduler but at the expense of greater overall disruption and higher computational cost, especially in complex, multi-scheduler scenarios.

Figure 3a displays two plots showing the percent change in Δ and Z compared to the baseline ($\alpha = 0$) for a representative instance as a function of the fairness level (various values of using α). Figure 3b displays a stacked area chart showing the distribution of changes from Stage 2 across



(a) Trade-off Between Efficiency and Fairness



(b) Burden Reallocation Across Schedulers

Figure 3: Side-by-side Comparison of Efficiency/Fairness Trade-off and Burden reallocation with α

eight schedulers as a function of the fairness level (various values of using α). The y-axis shows the percentage of total changes allocated to each scheduler. Each colored band corresponds to a specific scheduler. The width of each band at any fairness level reflects that scheduler's share of the total changes at that level of fairness. The x-axis represents increasing fairness levels (from 0.0 to 1.0).

As fairness increases, the reduction in the number of maximum changes by schedulers increases to reach around 17.3% while maintaining the same number of total changes. However, beyond a threshold ($\alpha = 0.75$), the total number of changes increases significantly while ensuring a slight increase in the reduction in the number of maximum changes by schedulers. This shift reflects a redistribution of changes toward a more equitable allocation. Initially, scheduler 2 dominates with over 45% of changes at the lowest fairness level, indicating high inequality in burden. However, its share declines significantly as fairness rises, while underutilized schedulers such as scheduler 1 and scheduler 3 gain a larger share. This shift reflects a redistribution of changes toward a more equitable allocation. The chart clearly shows how incorporating fairness into the objective leads to a more even distribution of scheduling changes among schedulers.

In addition to the Minimax metric, the analysis incorporates a fairness measure derived from the Gini coefficient (Chen and Hooker, 2023). A detailed formulation and additional experimental

Class	# Sched.	I ₀	I [*]	Without ML		With ML		GainA	GainT
				Arcs	Time	Arcs	Time		
1	2	4236	3444	138992	8.94	48971	1.02	64.77%	75.17%
2	5	10644	8357	462500	58.70	127236	3.13	75.03%	91.12%
3	8	18370	14709	893028	137.19	206595	5.53	76.87%	92.24%
4	11	22733	17667	1278907	277.74	278858	7.61	78.20%	94.77%
5	15	28879	22863	1816934	866.41	189891	9.57	89.55%	98.90%
6	20	40799	32641	3004375	3468.60	270678	13.19	90.99%	98.93%
7	30	58630	47863	5259231	-	401788	19.77	92.36%	98.96%
8	40	78488	65655	8341357	-	562008	26.48	93.26%	98.97%

Table 4.7: ML Impact Stage 1

results using this Gini metric are provided in Appendix B.

4.5 ML Impact

The ML component has a significant impact on the computational performance presented above. Table 4.7 illustrates the statistics for Stage 1, comparing scenarios with and without ML, and using the top-5 equipment suggestions provided by the ML model for each arc. Without ML, most instances in Classes 30 and 40 could not be solved. Furthermore, by learning from historical data, ML reduces the number of arcs by approximately 83%, which enables the solver to prove optimality on the reduced problem in cases where this was not possible otherwise and leads to a 94% reduction in execution time. Similarly to Stage 1, ML reduces the number of arcs considered by the Stage 2 models by approximately 75%, leading to a substantial 90% reduction in execution time, and improves the solver’s ability to close optimality gaps. The ML component, therefore, does not alter the optimal solution of the original OR model; instead, it identifies a smaller and more relevant decision space that allows the solver to reach optimality more consistently and more efficiently on the reduced problem.

To evaluate the benefits of the proposed dynamic top- κ_a mechanism, the comparison is made with a traditional static top- κ approach, in which a fixed κ value is applied uniformly across all arcs in a full network comprising 50 schedulers, 8000 nodes, and 24 million arcs. Figure 4 illustrates how optimality gap, arc reduction, and runtime execution vary with static $\kappa \in \{1, 5\}$. The analysis highlights the trade-offs between solution quality and computational efficiency: smaller κ values yield faster but suboptimal solutions (e.g., 9.72% optimality gap for $\kappa = 1$), whereas larger κ values

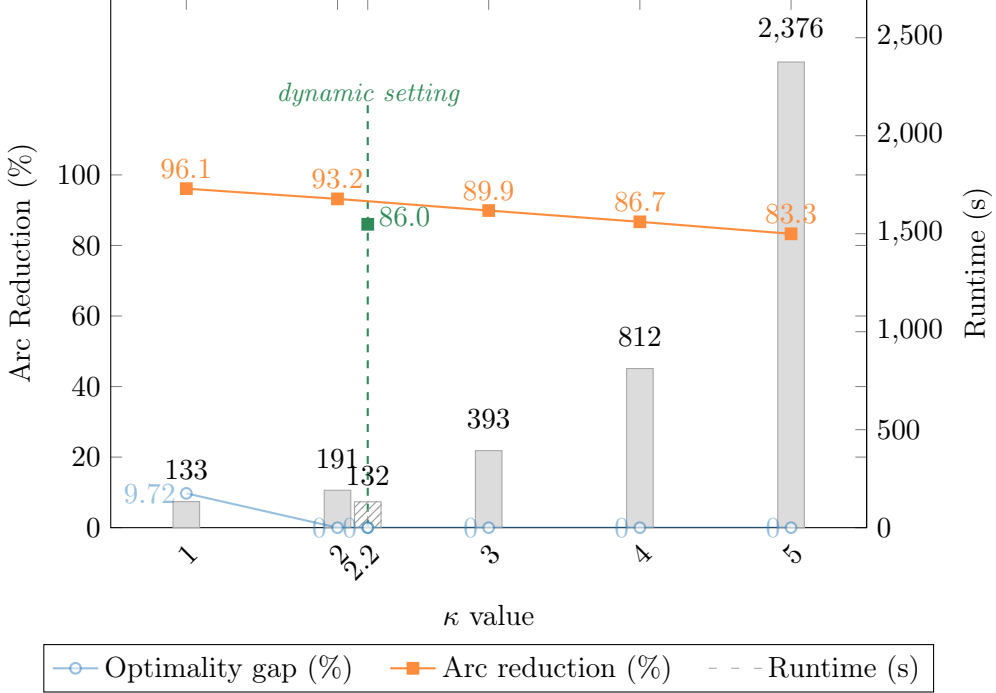


Figure 4: Dynamic- κ versus Static- κ

achieve optimal solutions at the expense of increased computation time. On the full network, when $\kappa = 5$, the solution is optimal, but the solver takes 2376 seconds.

The dynamic κ_a results, shown in green in Figure 4, correspond to the adaptive mechanism in which each arc is assigned its own κ_a based on the betweenness metric. The lone green point in the figure, with κ set to 2.2, is the weighted average of κ_a in the full network instance. Under this dynamic rule, the runtime is approximately 132 seconds, the arc reduction is 86.00%, and the solution remains optimal.

Results highlight how adapting κ_a to arc betweenness centrality affects the scalability of the OR models and the quality of the resulting substitution plans. Indeed, this adaptive mechanism tailors the search space to the local network structure, enhancing scalability and computational efficiency without compromising solution quality. By dynamically assigning values of κ to arcs based on the betweenness degree, this allows larger-scale networks to retain optimality while achieving runtimes consistent with smaller instances that rely on a static κ .

4.6 Managerial Insights

The results highlight a fundamental trade-off in resource substitution: optimizing solely for efficiency (e.g., minimizing total changes) can lead to unequal distribution of workload among schedulers. While such solutions are efficient from an optimization perspective, they may disproportionately burden certain schedulers, which in practice can result in partial implementation of recommendations, as some changes exceed what schedulers are willing or able to accommodate. Conversely, incorporating fairness into the objective promotes a more equitable distribution of tasks, often with only a modest increase in cost or computational effort. This substantially reduces disparities among schedulers, demonstrating that fairness-aware optimization can produce solutions that remain operationally sound while greatly improving workforce satisfaction and sustainability.

Importantly, incorporating fairness transforms the solution space from a single optimal point into a rich portfolio of efficient-fair solutions. Weighted-objective models allow decision-makers to balance efficiency and fairness, generating a Pareto frontier from which schedulers can select the most suitable solution for their operational context. For example, a company may accept a slight increase in total cost or complexity to achieve a fairer distribution of workload, particularly during peak periods or volatile conditions. This approach supports human-centered decision-making, where long-term resilience and employee satisfaction outweigh marginal efficiency gains.

The Pareto frontier of a representative instance is visualized in Figure 5. Adopting a 60% minimax fairness objective ($\alpha = 0.6$) results in a substantial rebalancing of workload without any loss in global solution quality. Specifically, the burden on the most-impacted scheduler decreases by 42% from 732 to 425. This demonstrates that substitution can be effectively redistributed to less-burdened neighbors without a trade-off.

In practice, the friction of coordinating among schedulers means that only a fraction of recommended changes are ever implemented, a setting referred to here as *partial implementation*, where schedulers adopt only the top-priority substitutions rather than the full set. As simulated in Figure 5, this is where the fair solution excels. When prioritizing and implementing only the highest-impact substitutions, the fair solution yields a greater reduction in system imbalance. This occurs because the fair algorithm had already allocated high-value changes more evenly across all

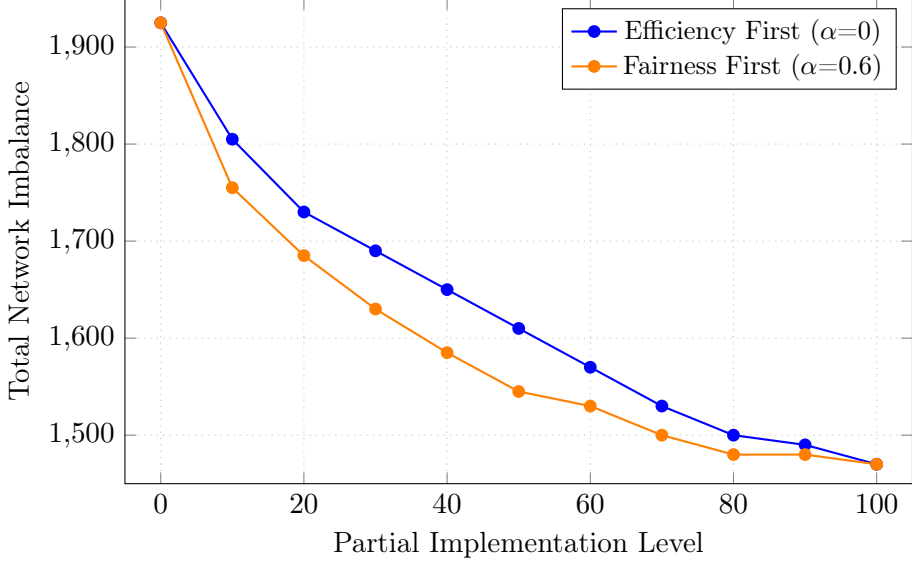


Figure 5: Comparison between the Pareto Frontiers for Efficiency and Fairness under a Partial Implementation Strategy

schedulers, making fair partial implementation a more effective strategy.

Another important aspect to highlight is that the degree of collaboration among schedulers, defined as the extent to which schedulers share resources and coordinate substitutions across different regions, has a pronounced impact on both computational performance and fairness outcomes. When schedulers collaborate extensively across regions, the resulting network exhibits strong inter-regional connectivity, enabling flexible resource sharing and more balanced workload distributions. In contrast, limited collaboration results in a fragmented structure with few inter-regional exchanges, thereby constraining adaptability and reinforcing local imbalances. As collaboration increases, the model can redistribute substitutions more evenly, leading to fairer and more stable solutions across the network. These findings underscore that collaborative flexibility is a key driver of fairness and efficiency in large-scale resource allocation systems.

5 Conclusion

Ensuring that the right resource is available at the right location and time remains a critical challenge in large-scale logistics networks, largely due to persistent imbalances arising from fluctuating demand and dynamic product flows. This paper addresses the NP-hard resource substitution problem by proposing a generic hybrid framework that integrates operations research and machine

learning. The framework explicitly models operational constraints, incorporates fairness considerations to align centralized plans with decentralized scheduler preferences, and leverages historical data to guide and accelerate the search for high-quality solutions. Applied to the network of one of the largest package delivery companies in the world, the framework demonstrated superior performance relative to existing substitution-based methods, achieving both computational efficiency and practical relevance. Beyond package delivery, the approach is broadly applicable to a wide range of resource balancing problems in transportation and logistics networks, including container repositioning, fleet assignment, and bike-sharing rebalancing. Future research directions include incorporating stochastic demand and supply uncertainties, exploring adaptive online learning approaches, and developing distributed implementations to further enhance scalability and operational flexibility in large-scale, real-time settings.

Acknowledgments

This research was partly supported by the NSF AI Institute for Advances in Optimization (Award 2112533).

References

Abrache, J., Crainic, T. G., and Gendreau, M. (1999). New decomposition algorithm for the deterministic dynamic allocation of empty containers.

Akhlaghi, V. E., Zandehshahvar, R., and Van Hentenryck, P. (2025). Propel: Supervised and reinforcement learning for large-scale supply chain planning. *arXiv preprint arXiv:2504.07383*.

ATRI (2024). An analysis of the operational costs of trucking: 2024 update. *ATRI Research Report*. Available at <https://truckingresearch.org/wp-content/uploads/2024/06/ATRI-Operational-Cost-of-Trucking-06-2024.pdf>.

Bengio, Y., Lodi, A., and Prouvost, A. (2021). Machine learning for combinatorial optimization: A methodological tour d'horizon. *European Journal of Operational Research*, 290(2):405–421.

Bertsimas, D., Farias, V. F., and Trichakis, N. (2011). The price of fairness. *Operations Research*, 59(1):17–31.

Bruglieri, M., Colorni, A., and Lue, A. (2014). The vehicle relocation problem for the one-way electric vehicle sharing: an application to the Milan case. *Procedia-Social and Behavioral Sciences*, 111:18–27.

Chen, V. X. and Hooker, J. N. (2022). Fairness through social welfare optimization. *arXiv preprint arXiv:2102.00311*.

Chen, V. X. and Hooker, J. N. (2023). A guide to formulating fairness in an optimization model. *Annals of Operations Research*, 326(1):581–619.

Chung, H., Freund, D., and Shmoys, D. B. (2018). Bike angels: An analysis of Citi Bike’s incentive program. In *Proceedings of the 1st ACM SIGCAS Conference on Computing and Sustainable Societies*, pages 1–9.

Crainic, T. G., Gendreau, M., and Dejax, P. (1993). Dynamic and stochastic models for the allocation of empty containers. *Operations research*, 41(1):102–126.

Dell’Amico, M., Hadjicostantinou, E., Iori, M., and Novellani, S. (2014). The bike sharing rebalancing problem: Mathematical formulations and benchmark instances. *Omega*, 45:7–19.

Desaulniers, G., Desrosiers, J., and Solomon, M. M. (2006). *Column generation*, volume 5. Springer Science & Business Media.

Du, Y. and Hall, R. (1997). Fleet sizing and empty equipment redistribution for center-terminal transportation networks. *Management Science*, 43(2):145–157.

Er Raqabi, E. M., Beljadid, A., Bennouna, M. A., Bennouna, R., Boussaadi, L., El Hachemi, N., El Hallaoui, I., Fender, M., Jamali, M. A., Si Hammou, N., et al. (2025). OCP optimizes its supply chain for Africa. *INFORMS Journal on Applied Analytics*, 55(6):437–456.

Er Raqabi, E. M., El Hallaoui, I., and Soumis, F. (2023a). The Primal Benders Decomposition. *Les Cahiers du GERAD*, G-2023-27.

Er Raqabi, E. M., Himmich, I., El Hachemi, N., El Hallaoui, I., and Soumis, F. (2023b). Incremental LNS framework for integrated production, inventory, and vessel scheduling: Application to a global supply chain. *Omega*, 116:102821.

Er Raqabi, E. M., Wu, Y., El Hallaoui, I., Soumis, F., et al. (2024). Towards resilience: Primal large-scale re-optimization. *Transportation Research Part E: Logistics and Transportation Review*, 192:103819.

Erera, A. L., Morales, J. C., and Savelsbergh, M. (2005). Global intermodal tank container management for the chemical industry. *Transportation Research Part E: Logistics and Transportation Review*, 41(6):551–566.

Erera, A. L., Morales, J. C., and Savelsbergh, M. (2009). Robust optimization for empty repositioning problems. *Operations Research*, 57(2):468–483.

Freund, D., Henderson, S. G., and Shmoys, D. B. (2022). Minimizing multimodular functions and allocating capacity in bike-sharing systems. *Operations Research*, 70(5):2715–2731.

Ghosh, S., Varakantham, P., Adulyasak, Y., and Jaillet, P. (2017). Dynamic repositioning to reduce lost demand in bike sharing systems. *Journal of Artificial Intelligence Research*, 58:387–430.

Goodfellow, I., Bengio, Y., and Courville, A. (2016). *Deep learning*. MIT press.

Gupta, S., Moondra, J., and Singh, M. (2023). Which LP norm is the fairest? approximations for fair facility location across all “p”. *Proceedings of the 24th ACM Conference on Economics and Computation*, page 817.

Himmich, I., El Hachemi, N., El Hallaoui, I., Metrane, A., Soumis, F., et al. (2023). MPILS: An automatic tuner for MILP solvers. *Computers & Operations Research*, 159:106344.

Jansen, B., Swinkels, P. C., Teeuwen, G. J., de Fluiter, B. v. A., and Fleuren, H. A. (2004). Operational planning of a large-scale multi-modal transportation system. *European Journal of Operational Research*, 156(1):41–53.

Jarrah, A. I., Goodstein, J., and Narasimhan, R. (2000). An efficient airline re-fleeting model for the incremental modification of planned fleet assignments. *Transportation Science*, 34(4):349–363.

Karsu, Ö. and Morton, A. (2015). Inequity averse optimization in operational research. *European Journal of Operational Research*, 245(2):343–359.

Kingma, D. P. and Ba, J. (2015). Adam: A method for stochastic optimization. In *3rd International Conference on Learning Representations, ICLR 2015, San Diego, CA, USA, May 7-9, 2015, Conference Track Proceedings*.

LeCun, Y., Bengio, Y., and Hinton, G. (2015). Deep learning. *nature*, 521(7553):436–444.

Lendon, C. and Wrathall, E. (1967). Scheduling empty freight car fleets on the Louisville and Nashville railroad. In *Second International Symposium on the Use of Cybernetics on the Railways*, pages 1–6.

Leslie, A. and Murray, D. (2024). An analysis of the operational costs of trucking: 2024 update.

Li, Y., Zheng, Y., and Yang, Q. (2018). Dynamic bike reposition: A spatio-temporal reinforcement learning approach. In *Proceedings of the 24th ACM SIGKDD International Conference on Knowledge Discovery & Data Mining*, pages 1724–1733.

Lin, D.-Y., Lee, Y.-J., and Lee, Y. (2015). The container retrieval problem with respect to relocation. *Transportation Research Part C: Emerging Technologies*, 52:132–143.

Lodi, A., Sankaranarayanan, S., and Wang, G. (2024). A framework for fair decision-making over time with time-invariant utilities. *European Journal of Operational Research*, 319(2):456–467.

Long, Y., Lee, L. H., and Chew, E. P. (2012). The sample average approximation method for empty container repositioning with uncertainties. *European Journal of Operational Research*, 222(1):65–75.

López-Ibáñez, M., Dubois-Lacoste, J., Cáceres, L. P., Birattari, M., and Stützle, T. (2016). The irace package: Iterated racing for automatic algorithm configuration. *Operations Research Perspectives*, 3:43–58.

Lourenço, H. R., Martin, O. C., and Stützle, T. (2003). Iterated local search. In *Handbook of metaheuristics*, pages 320–353. Springer.

Lv, C., Zhang, C., Lian, K., Ren, Y., and Meng, L. (2020). A hybrid algorithm for the static bike-sharing re-positioning problem based on an effective clustering strategy. *Transportation Research Part B: Methodological*, 140:1–21.

Misra, S. (1972). Linear programming of empty wagon disposition. *Rail International*, 3(3).

Morabit, M., Desaulniers, G., and Lodi, A. (2023). Machine-learning-based arc selection for constrained shortest path problems in column generation. *INFORMS Journal on Optimization*, 5(2):191–210.

Morabit, M., Zarpellon, G., Lodi, A., Bengio, Y., Gaudreault, J., and Rousseau, L.-M. (2021). Machine-learning-based column selection for column generation. *Transportation Science*, 55(4):815–831.

Nair, R. and Miller-Hooks, E. (2011). Fleet management for vehicle sharing operations. *Transportation Science*, 45(4):524–540.

Newman, M. (2018). *Networks*. Oxford University Press.

Powell, W. B. (1986). A stochastic model of the dynamic vehicle allocation problem. *Transportation science*, 20(2):117–129.

Powell, W. B. (1987). An operational planning model for the dynamic vehicle allocation problem with uncertain demands. *Transportation Research Part B: Methodological*, 21(3):217–232.

Quesnel, F., Wu, A., Desaulniers, G., and Soumis, F. (2022). Deep-learning-based partial pricing in a branch-and-price algorithm for personalized crew rostering. *Computers & Operations Research*, 138:105554.

Scavuzzo, L., Aardal, K., Lodi, A., and Yorke-Smith, N. (2024). Machine learning augmented branch and bound for mixed integer linear programming. *Mathematical Programming*, pages 1–44.

Schuijbroek, J., Hampshire, R. C., and Van Hoeve, W.-J. (2017). Inventory rebalancing and vehicle routing in bike sharing systems. *European Journal of Operational Research*, 257(3):992–1004.

Shu, J., Chou, M. C., Liu, Q., Teo, C.-P., and Wang, I.-L. (2013). Models for effective deployment and redistribution of bicycles within public bicycle-sharing systems. *Operations Research*, 61(6):1346–1359.

Song, D.-P. (2005). Optimal threshold control of empty vehicle redistribution in two depot service systems. *IEEE Transactions on Automatic Control*, 50(1):87–90.

Tahir, A., Quesnel, F., Desaulniers, G., El Hallaoui, I., and Yaakoubi, Y. (2021). An improved integral column generation algorithm using machine learning for aircrew pairing. *Transportation Science*, 55(6):1411–1429.

White, W. W. (1972). Dynamic transshipment networks: An algorithm and its application to the distribution of empty containers. *Networks*, 2(3):211–236.

Xie, Y., Liang, X., Ma, L., and Yan, H. (2017). Empty container management and coordination in intermodal transport. *European Journal of Operational Research*, 257(1):223–232.

Yang, Y., Ridouane, Y., Boland, N., Erera, A., and Savelsbergh, M. (2022). Substitution-based equipment balancing in service networks with multiple equipment types. *European Journal of Operational Research*, 300(3):966–978.

Yu, J., Liu, P., Lu, X., and Gu, M. (2025). Analyzing the price of fairness in scheduling problems with two agents. *European Journal of Operational Research*, 321(3):750–759.

Appendix A Compatibility Matrix Package Delivery Company

The company employs different types of equipment in its ground transportation network, both trailers and containers, which are grouped into categories based on their size: shorts (trailers with a length of 28 feet), longs (trailers with a length ranging from 40 to 48 feet), and extra longs (trailers with a length of 53 feet).

	r_1	r_2	r_3	r_4	r_5	r_6	r_7	r_8	r_9	r_{10}	r_{11}	r_{12}	r_{13}	r_{14}
r_1	1	1	1	1	0	0	0	0	0	0	0	0	0	0
r_2	1	1	1	1	0	0	0	0	0	0	0	0	0	0
r_3	1	1	1	1	0	0	0	0	0	0	0	0	0	0
r_4	1	1	1	1	1	0	0	0	0	0	0	0	0	1
r_5	1	1	1	1	1	0	0	0	0	0	0	0	0	1
r_6	1	1	1	1	1	1	0	0	0	0	0	0	0	1
r_7	1	1	1	1	1	1	1	0	0	0	0	0	0	1
r_8	1	1	1	1	1	1	1	1	0	0	0	0	0	1
r_9	1	1	1	1	1	1	1	1	1	0	0	0	0	1
r_{10}	1	1	1	1	1	1	1	1	1	1	0	0	0	1
r_{11}	1	1	1	1	1	1	1	1	1	1	1	0	0	1
r_{12}	0	0	0	0	0	0	0	0	0	0	0	1	0	0
r_{13}	1	1	1	1	1	1	1	1	1	1	1	0	1	1
r_{14}	1	1	1	1	1	1	1	1	1	1	1	0	1	1

Table A.1: Equipment Allowable Substitution Matrix

Equipment types can be combined into composite types. For example, a common composite type is a combination of two shorts pulled by a single truck tractor. Other composite types are three shorts or a long combined with a short. In general, the equipment assigned to a load can be substituted by a larger type as long as the origin and destination facility of the load can accommodate the new type.

Appendix B Gini Model

An alternative approach to the Minimax metric is to use a metric inspired by the Gini coefficient to promote equality across the entire distribution of scheduler burdens. This avoids focusing only on the single most-burdened scheduler and instead seeks to minimize the total pairwise inequality.

A hybrid model combining this Gini-based metric with the utilitarian objective of minimizing total changes can be formulated. Let the burden for each scheduler $s \in \mathcal{S}$, denoted B_s , be the total

number of changes assigned to it:

$$B_s = \sum_{a \in \mathcal{A}_s} (1 - x_a \Phi_0(a)), \quad (\text{B.1})$$

where \mathcal{A}_s is defined as in the Minimax model, representing the set of arcs under the responsibility of scheduler s , x_a is the binary decision variable indicating whether arc a is kept ($x_a = 1$) or removed ($x_a = 0$), and $\Phi_0(a)$ denotes the original arc assignment.

The Stage 2 model becomes:

$$\Delta^{fair} = \min (1 - \omega) \sum_{s \in \mathcal{S}} B_s + \omega \sum_{\substack{s_1, s_2 \in \mathcal{S} \\ s_1 < s_2}} |B_{s_1} - B_{s_2}| \quad (\text{B.2})$$

$$\text{s.t. } \sum_{n \in \mathcal{N}} \sum_{r \in \mathcal{R}} I_{nr} \leq I^*, \quad (\text{B.3})$$

Constraints (3.3) to (3.6).

where $\omega \in [0, 1]$ is a weight parameter that controls the trade-off between overall efficiency (minimizing total changes, when $\omega = 0$) and fairness (minimizing the sum of absolute differences, when $\omega = 1$). The term $\sum |B_{s_1} - B_{s_2}|$ is directly proportional to the Gini coefficient of the burden distribution.

To linearize the model, introduce continuous difference variables $D_{s_1 s_2}$ to represent the absolute differences between pairs of scheduler burdens:

$$\Delta^{fair} = \min (1 - \omega) \sum_{s \in \mathcal{S}} B_s + \omega \sum_{\substack{s_1, s_2 \in \mathcal{S} \\ s_1 < s_2}} D_{s_1 s_2} \quad (\text{B.4})$$

$$\text{s.t. } B_s = \sum_{a \in \mathcal{A}_s} (1 - x_a \Phi_0(a)), \quad \forall s \in \mathcal{S}, \quad (\text{B.5})$$

$$D_{s_1 s_2} \geq B_{s_1} - B_{s_2}, \quad \forall s_1 < s_2, \quad (\text{B.6})$$

$$D_{s_1 s_2} \geq B_{s_2} - B_{s_1}, \quad \forall s_1 < s_2, \quad (\text{B.7})$$

Constraints (3.3) to (3.6), (B.3).

In addition to the minimax metric, tests are also conducted using the Gini index. Table B.1

compares the three strategies: Efficiency (minimizing total changes), Fairness (minimax), and Gini (minimizing inequality in changes using the Gini index). The results reveal distinct trade-offs between the three models. For all classes, the Fairness and Gini approaches yield better results. The Z metric significantly decreases compared to the Efficiency approach. However, the Δ^{FAIR} significantly increases compared to the Δ^{GINI} , which remains closer to Δ .

Class	# Sched.	I_0	I_*	Efficiency			Fairness			Fairness Gini		
				Δ^*	Z^*	Time	Δ^{FAIR}	Z^{FAIR}	Time	Δ^{GINI}	Z^{GINI}	Time
1	2	4236	3444	321	199	1.44	357	188	1.53	336	204	1.40
2	5	10644	8357	952	354	4.74	1135	242	5.50	1085	286	8.42
3	8	18370	14709	1542	452	8.27	1852	274	11.30	1829	318	23.80
4	11	22733	17667	2048	443	12.25	2796	285	15.50	2563	330	49.5
5	15	28879	22863	2701	486	15.14	4184	308	18.16	3344	312	104.80
6	20	40799	32641	3725	710	22.13	7350	397	24.98	5149	400	88.71
7	30	58630	47863	4941	688	34.99	9039	331	39.65	7193	336	146.65
8	40	78488	65655	5943	732	44.33	13510	394	53.11	9237	397	209.02

Table B.1: Stage 2 for the Gini Model

Computation times highlight another key difference. While Efficiency and Fairness remain computationally reasonable for all classes, the Gini model can be more expensive. For all classes, enforcing fairness through the Gini model significantly increases the execution time compared to the efficiency and minimax approaches. For example, in Class 8, runtime rises from 53.11 (Efficiency) to 209.02 (Gini index), while increasing Z from 394 to 397. This suggests that minimizing inequality is computationally challenging, especially for larger problems with more schedulers.

Figure 6 illustrates the effect of increasing the Gini weight (ω) on the distribution of changes among eight schedulers, expressed as a percentage of total changes. The x-axis represents the Gini weight ranging from 0.2 (low emphasis on fairness) to 1.0 (high emphasis on fairness), while the y-axis shows the percentage share of changes for each scheduler. The goal of applying the Gini index is to reduce inequality by ensuring a more balanced distribution of changes among schedulers.

At $\omega = 0.2$, the distribution is highly uneven, with Scheduler 4 dominating the share of total changes (close to 35–40%), while some schedulers, like 1 and 2, have relatively small shares (around 10% each). This indicates that when fairness is given little importance, a few schedulers absorb most disruptions, which minimizes overall cost but creates inequity. As ω increases to 0.5, the distribution

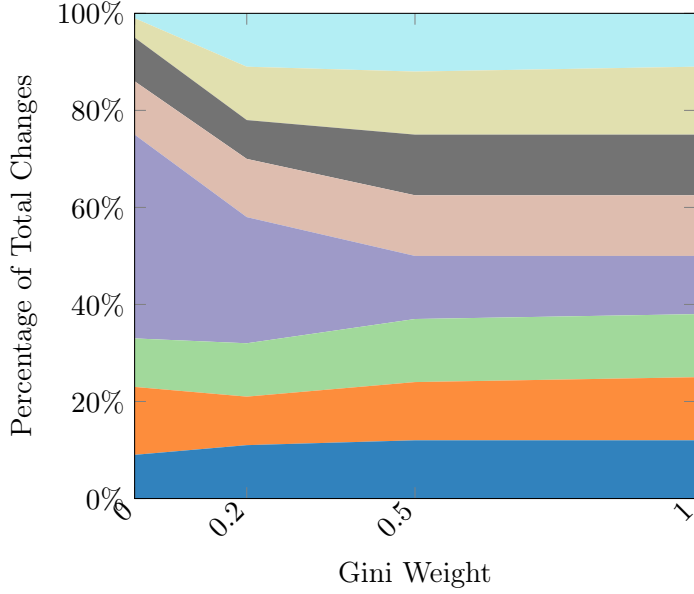


Figure 6: Weighted Models Gini

becomes noticeably more balanced: Scheduler 4’s share drops significantly, while Schedulers 1, 2, and 3 gain a larger proportion, suggesting that fairness constraints start redistributing changes from heavily burdened schedulers to those previously less affected.

By $\omega = 1.0$, the distribution appears relatively uniform, with all schedulers contributing between approximately 10% and 15% of total changes. This confirms that the Gini-based fairness mechanism successfully enforces equity among schedulers, preventing any single one from being disproportionately impacted. However, achieving this balanced state typically requires increasing the total number of changes, as seen in earlier tables, which means higher overall disruption. The trend demonstrates the trade-off managed by the Gini approach: it does not aim to minimize the maximum load (like minimax fairness) but reduces disparities across schedulers, leading to a more proportionate workload distribution at higher fairness weights.